Biomedical Optics EXPRESS

Fiber-optic OCT sensor guided "SMART" micro-forceps for microsurgery

Cheol Song,[1,*] Dong Yong Park,[2] Peter L. Gehlbach,[3] Seong Jin Park,[2] and Jin U. Kang[1]

[1]*Department of Electrical and Computer Engineering, Johns Hopkins University, 3400 N. Charles St., Baltimore, MD 21218, USA*
[2]*Department of Mechanical Engineering, POSTECH, Hyoja-dong, Pohang 790-784, Korea*
[3]*Wilmer Eye Institute, Johns Hopkins School of Medicine, 600 N. Wolfe St., Baltimore, MD 21287, USA*
**csong16@jhu.edu*

Abstract: A handheld Smart Micromanipulation Aided Robotic-surgery Tool (SMART) micro-forceps guided by a fiber-optic common-path optical coherence tomography (CP-OCT) sensor is presented. A fiber-optic CP-OCT distance and motion sensor is integrated into the shaft of a micro-forceps. The tool tip position is manipulated longitudinally through a closed loop control using a piezoelectric motor. This novel forceps design could significantly enhance safety, efficiency and surgical outcomes. The basic grasping and peeling functions of the micro-forceps are evaluated in dry phantoms and in a biological tissue model. As compared to freehand use, targeted grasping and peeling performance assisted by active tremor compensation, significantly improves micro-forceps user performance.

OCIS codes: (280.4788) Optical sensing and sensors; (170.3890) Medical optics instrumentation; (170.4500) Optical coherence tomography; (060.2370) Fiber optics sensors.

References and links

1. C. N. Riviere, J. Gangloff, and M. de Mathelin, "Robotic compensation of biological motion to enhance surgical accuracy," Proc. IEEE **94**(9), 1705–1716 (2006).
2. K. Ikuta, T. Kato, and S. Nagata, "Development of micro-active forceps for future microsurgery," Minim. Invasive Ther. Allied Technol. **10**(4-5), 209–213 (2001).
3. T. Kawai, K. Nishizawa, F. Tajima, K. Kan, M. Fujie, K. Takakura, S. Kobayashi, and T. Dohi, "Development of exchangeable microforceps for a micromanipulator system," Adv. Robot. **15**(3), 301–305 (2001).
4. J.-P. Hubschman, J.-L. Bourges, W. Choi, A. Mozayan, A. Tsirbas, C.-J. Kim, and S.-D. Schwartz, "'The Microhand': a new concept of micro-forceps for ocular robotic surgery," Nat. Eye **24**(2), 364–367 (2010).
5. X. He, M. A. Balicki, J. U. Kang, P. L. Gehlbach, J. T. Handa, R. H. Taylor, and I. I. Iordachita, "Force sensing micro-forceps with integrated fiber Bragg grating for vitreoretinal surgery," Proc. SPIE **8218**, 82180W, 82180W-7 (2012).
6. I. Kuru, B. Gonenc, M. Balicki, J. Handa, P. Gehlbach, R. H. Taylor, and I. Iordachita, "Force sensing micro-forceps for robot assisted retinal surgery," in *Proceedings of IEEE Conference on Engineering in Medicine and Biology Society* (Institute of Electrical and Electronics Engineers, San Diego, 2012), pp.1401–1404.
7. K. Zhang, W. Wang, J. Han, and J. U. Kang, "A surface topology and motion compensation system for microsurgery guidance and intervention based on common-path optical coherence tomography," IEEE Trans. Biomed. Eng. **56**(9), 2318–2321 (2009).
8. J. U. Kang, J. H. Han, X. Liu, and K. Zhang, "Common-path optical coherence tomography for biomedical imaging and sensing," J. Opt. Soc. Korea **14**(1), 1–13 (2010).
9. J. U. Kang, J. H. Han, X. Liu, K. Zhang, C. G. Song, and P. Gehlbach, "Endoscopic functional Fourier domain common path optical coherence tomography for microsurgery," IEEE J. Sel. Top. Quantum Electron. **16**(4), 781–792 (2010).
10. C. Song, P. L. Gehlbach, and J. U. Kang, "Active tremor cancellation by a 'smart' handheld vitreoretinal microsurgical tool using swept source optical coherence tomography," Opt. Express **20**(21), 23414–23421 (2012).
11. Y. Huang, X. Liu, C. Song, and J. U. Kang, "Motion-compensated hand-held common-path Fourier-domain optical coherence tomography probe for image-guided intervention," Biomed. Opt. Express **3**(12), 3105–3118 (2012).

#189235 - $15.00 USD Received 22 Apr 2013; revised 4 Jun 2013; accepted 4 Jun 2013; published 4 Jun 2013

1. Introduction

Safely and efficiently performing retinal microsurgery requires accurate and precise tool tip control. This is facilitated by reduction of physiological hand tremor that predominate in a frequency band of about 6 - 12 Hz, with on the order of 100 μm of motion that is neither task directed nor intended [1]. At the present time, highly skilled retinal surgeons complete basic microsurgical objectives by employing high levels of concentration, dexterity and fine motor control, bringing years of training and experience to bear on the defined motor task. Today, the peeling of micron scale membranes from the delicate retinal surface, without damaging its fragile neurons, is usually accomplished with unassisted freehand tools, typically a micro-forceps. Attempts to improve the micro-forceps have included but not been limited to, built-in fiberscope and end-effectors to assist in retinal surgery tasks [2]; miniaturization and use of exchangeable micro-forceps as a part of micromanipulation system to assist in minimally invasive surgery [3]; MEMS technology has also been applied to the development of micro-forceps for intraocular surgery [4]. Recently, a force sensing, fiber Bragg grating based micro-forceps to provide force feedback during vitreoretinal surgery has been presented [5,6]. Over the last decade optical coherence tomography (OCT) has emerged as a dominant diagnostic imaging modality in clinical ophthalmology. Nevertheless its application as a potential sensor for intraoperative tool control is fairly new [7–9]. We have recently presented a novel microsurgical tool platform, SMART (Smart Micromanipulation Aided Robotic-surgery Tool) and have demonstrated its ability to cancel a surgeon's physiological tremor [10] and to stabilize a handheld imaging probe [11]. SMART instruments utilize common path, swept source optical coherence tomography (CP SS-OCT) in closed loop with a piezoelectric motor based feedback control system. Active tremor reduction of the SMART is achieved by positioning and by continuously and rapidly repositioning the tool tip at a defined constant offset distance from the sample surface by using the piezoelectric motor response to the distance sensing function of the SS-OCT. The sensor response function of the tool prevents unintended tissue contact and damage, stabilizes tool tip tremor and allows steady positioning of the tool tip at previously unsustainable distances from the target tissue. In this work we extend the SMART platform to the more complicated functions of the micro-forceps. Data comparing the freehand and SMART assisted micro-forceps functions of grasping and peeling are evaluated, in both dry and wet phantoms. The significantly enhanced performance of the SMART micro-forceps is presented.

2. SMART micro-forceps system

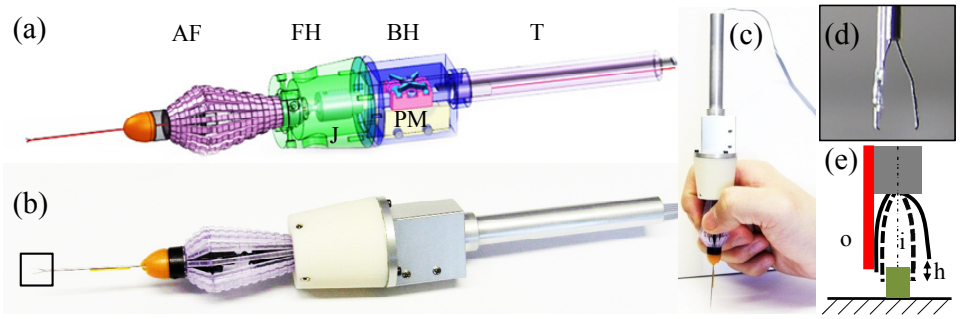

Fig. 1. Handheld SMART micro-forceps for microsurgery. (a) CAD cross-sectional image AF: Alcon forceps, FH: front holder, BH: back holder, J: joint, T: tail, PM: piezoelectric motor. (b) Photo image of the implemented SMART micro-forceps prototype. (c) Handheld SMART micro-forceps. (d) A magnified view of optical fiber attached to the finger of the micro-forceps (b), (e) The asymmetric configuration of two fingers, i and o: inside and outside of the fingers, h: height error during grasping, red line (optical fiber), full line (open grasp), dotted line (closed grasp).

#189235 - $15.00 USD Received 22 Apr 2013; revised 4 Jun 2013; accepted 4 Jun 2013; published 4 Jun 2013

A fiber-optic CP SS-OCT is designed for precision distance sensing. This is combined with an active surgical tool tip (micro-forceps) capable of high-speed precise axial motion to form the basis of SMART tool platform. The OCT sensor assesses tool tip motion relative to the target and compensates for unwanted and unintended tremor, using a high speed piezoelectric motor (LEGS-LL1011A, PiezoMotor) connected to the tool tip. Figure 1(a) shows a CAD rendering of the SMART micro-forceps; Fig. 1(b) shows a photograph of the assembled SMART micro-forceps; Fig. 1(c) demonstrates the SMART micro-forceps in use; Fig. 1(d) shows an enlarged view of the single mode fiber glued to one "finger" of the forceps. Of further practical note, in this prototype instrument the optical fiber is glued along the outside of the forceps fingers (Fig. 1(e), "o") to avoid artifact signals generated by the tissue edge at the time of grasping. The illustrated prototype incorporates a commercially available but highly customized reusable micro-forceps (Alcon,Inc., Fort Worth, TX) commonly used in vitreoretinal surgery. Manual action occurs by compressing thin-walled plastic ribs comprising its body, the outer needle of the Alcon forceps then moves forward to engage the two "finger tips" of the forceps. The inner needle inclusive of the forceps fingers, was carefully modified to move freely and to be connected to the drive rod of a PZT motor. The motor has a maximum speed of 15 mm/s, a resolution of less than 1 nm, and the maximum micro-stepping frequency from the motor controller (PMD90) is 125 kHz. The configuration of the forceps fingers was asymmetrically modified to reduce an inherent height error (Fig. 1(e), "h") resulting from the movement arc of the fingers. In the presented prototype the single-mode fiber that is used as a high-speed distance sensor and is simply attached to the relatively straight finger of the forcep.

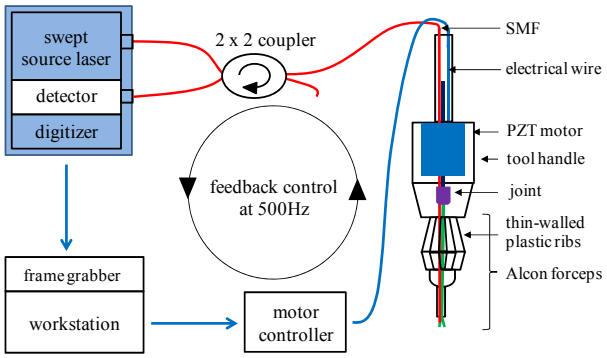

Fig. 2. Schematic of the SMART micro-forceps based on CP SS-OCT operating at the center wavelength of 1060 nm and feedback control scheme at an update speed of 500 Hz.

Figure 2 illustrates SMART micro-forceps configuration. A swept source optical coherence tomography (SS-OCT) system and a PZT motor controller are connected to a quad-core workstation (Dell, T7500). The SS-OCT has a swept source OEM engine (AXSUN, $\lambda_0 = 1060\ nm$, sweeping rate = 100 kHz, 3 dB axial resolution = 8 µm, scan range = 3.7 mm in air), a 2 x 2 coupler, a photodetector and a digitizer with a sampling rate of up to 500 MSPS with 12 bit resolution. This SS-OCT engine has a Camera Link DAQ Board to handle OCT signals such as the SD-OCT signal, which is connected with a Camera Link frame grabber (National Instruments). A LabVIEW based OCT signal processing and feedback control scheme is currently used to update the closed-loop at 500 Hz through the workstation. The primary goal is to position the surgical micro-forceps' tip at a predetermined offset distance from the surgical target and to maintain that distance during the grasping movement, independent of surgeon and target motion. The motor compensation speed of 500 Hz is substantially higher than that required to compensate for a typical tremor frequency of 0 - 15 Hz. The regime of the proportional-integral-derivative (PID) feedback control is similar to that reported in our previous SMART system and includes: 1. surface detection of the target

#189235 - $15.00 USD Received 22 Apr 2013; revised 4 Jun 2013; accepted 4 Jun 2013; published 4 Jun 2013

sample using an OCT signal; 2. activation of tremor compensation; 3. action of micro-forceps grasping function. To engage both finger tips of the SMART micro-forceps, the relative position between the inner and the outer needle should be initialized prior to conducting a tremor compensation experiment. Even though the inner needle is capable of moving throughout the 3 mm effective OCT sensing range, the inner forceps' "finger" was stabilized while in SMART assisted mode to a movement range of 0.5 mm in order to allow safe manipulation.

3. Grasping function of SMART micro-forceps

We studied the grasping ability of the micro-forceps to maintain constant offset distances during handheld use in dry phantoms. An observable, quantifiable, and significant reduction in the effect of the physiological tremor of around 6 - 12 Hz at the tool tip is present in SMART assisted grasp in Fig. 3. There is also decrease of the low frequency band, on the order of 0 - 5 Hz that results in large amplitude instrument position drift. When analyzing the hand tremor of a retina surgeon the SMART micro-forceps system, enhanced with feedback control for real-time distance tracking, did effectively cancel unintended instrument drift, while the tremor compensation function provided tip stabilization throughout the grasping movement. The prototype SMART micro-forceps tested here was shown to be operative at tissue offset positions of up to a 3 mm effective OCT sensing distance from the target surface.

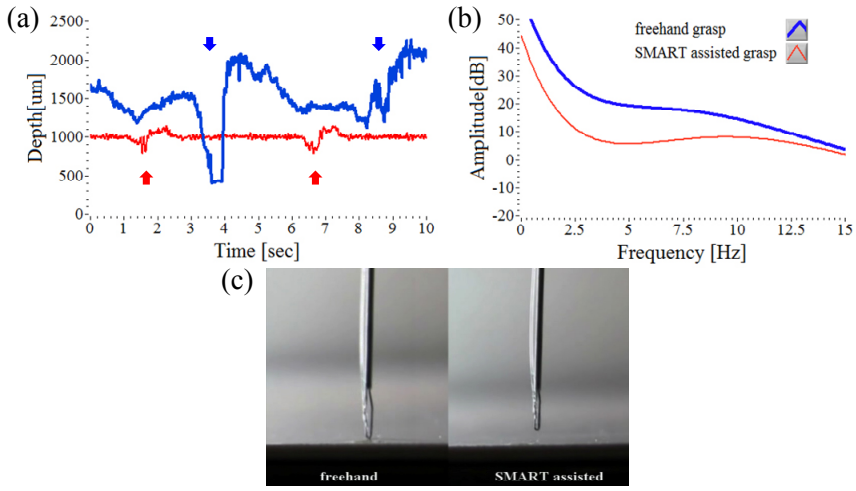

Fig. 3. Comparison of tool tip position relative to the target surface during freehand grasp (blue line) and SMART assisted grasp (red line) using a dry phantom (white paper). (a) Two attempts to grasp starting from a defined offset height of 1000 µm for 10 seconds. The arrows indicate the tip moment during grasp events. (b) The Fourier analysis of the two tip movement graphs, (a). (c) Real-time video image (Media 1) showing freehand grasp attempts and SMART assisted grasp attempts on a thick white paper.

Figure 3(a) shows 10 seconds of representative data captured during two attempts at freehand grasp, (blue line). This is compared to two attempts to grasp with the instrument assisted by tremor compensation, (red line). The comparative data clearly demonstrates a large difference in tool tip stability both when maintaining the offset position and during the grasping motion of the micro-forceps. In the case of freehand grasp, tool tip motion is on the order of 1000 µm directed towards the target surface. When assisted by tremor compensation, tool tip motion directed towards the target surface is generally less than 350 µm. Figure 3(b) shows averaged graphs of the Fourier analyses of up to 15 Hz from 5 data sets, with 20th order polynomial least-square fitting. The Fourier transformed amplitude of SMART assisted grasp data is less than that of freehand grasp data. While both unassisted and assisted grasping

#189235 - $15.00 USD Received 22 Apr 2013; revised 4 Jun 2013; accepted 4 Jun 2013; published 4 Jun 2013

motions direct the tool tip towards the target the amplitude reduction between the two Fourier transform data sets, as graphed, is relatively larger (10 dB) in the low frequency band (0 - 5 Hz) than in the high frequency band (10 - 15 Hz). Figure 3(c) is a representative video clip of every 5 second trial of real-time freehand grasping motion, and is compared to the SMART assisted tremor compensation. The video (Media 1) was played back at 30 fps. The video data of the tool tip during grasping, when assisted by tremor compensation, represents the potential for enhancing microsurgical safety and capability in the hands of a skilled micro-surgeon.

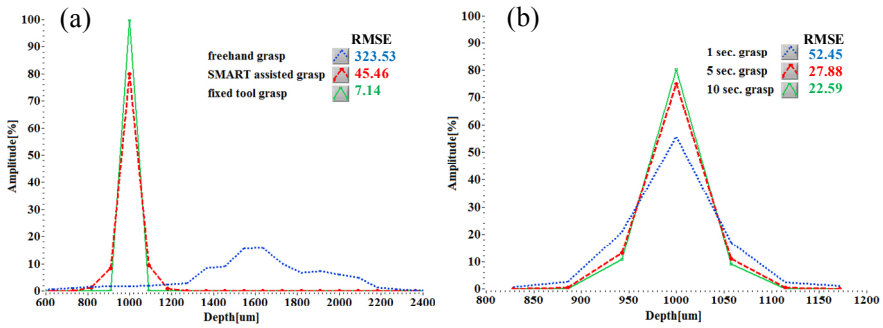

Fig. 4. Height histogram and RMSE of SMART micro-forceps in terms of grasp mode and grasp duration. (a) Height data analysis of the freehand, SMART assisted and in fixed position (two grasps for 10 seconds and one during 1 second) averaged from 5 data sets. (b) Height comparison according to three different durations of SMART assisted grasp, which are averaged from 10 data sets; 1 second and 5 second grasps indicate sustained grasping every 5 seconds; 10 second grasp indicates that the grasp was sustained over 10 seconds.

We assessed the grasp performance of the SMART micro-forceps using two different parameters: grasp type and grasp time. The intrinsic grasp error of the micro-forceps without any tremor was measured with tremor compensation on after firmly attaching it to a rigid body (tool position fixed). Figure 4(a) shows three histograms of the Root Mean Square Error (RMSE) of grasping under the three different experimental conditions (freehand, SMART assisted and fixed tool position with compensation on). The histogram graphs represent averaged data from 5 data sets. The height change associated with the tool stuck to a rigid post, RMSE of 7.14 is intrinsically present at baseline in the tremor compensated tool data and acts on its RMSE of 45.46. The narrow histogram in the SMART assisted grasp data supports the premise of improved tip control as compared to freehand use. The tool tip position of freehand grasp is by comparison highly variable in all ranges, particularly near 1600 μm. Freehand grasp may be inherently more difficult from an offset distance of 1000 μm. In Fig. 4(b), SMART assisted grasping performance with time constraints was evaluated. Increasing the time duration from 1 second to 5 seconds to grasp, decreased the RMSE of the action. Increasing the time to grasp to 10 seconds did not further reduce the RMSE a lot.

4. Peeling of biological membrane

Enhanced precision in micro-forceps peeling assisted by tremor compensation was also demonstrated in a biological tissue model, thereby further validating its potential as a practical microsurgical device. During the peeling of biological membranes (the inner and outer membrane of the egg shell), the SMART micro-forceps diminishes hand tremor but also enables the user to precisely place the tool tip at a distance suitable for grasping and peeling. For the assessment of micro-forceps peeling function the tough inner membrane was incised prior to grasping. And then black ink was applied to the edge of the membrane to show clarify the membrane boundaries. Figures 5(a) and 5(b) show the corresponding height signals and the Fourier analysis for both freehand and SMART assisted peeling tests, respectively. This result is also similar to those of previous grasp tests. Figure 5(c) is a representative video

#189235 - $15.00 USD Received 22 Apr 2013; revised 4 Jun 2013; accepted 4 Jun 2013; published 4 Jun 2013

frame of the freehand and SMART assisted peeling; the video (Media 2) runs at 30 fps. SMART assisted peeling with tremor compensation demonstrates improved performance without serious physical contact to the egg shell, however freehand peeling without the OCT depth assessment increased the difficulty of identifying the membrane edge for the user. During the egg membrane peeling experiment, the reflected OCT signal varies in strength due to the underlying curvature of the egg shell. This diminishes tool tip stability in this model.

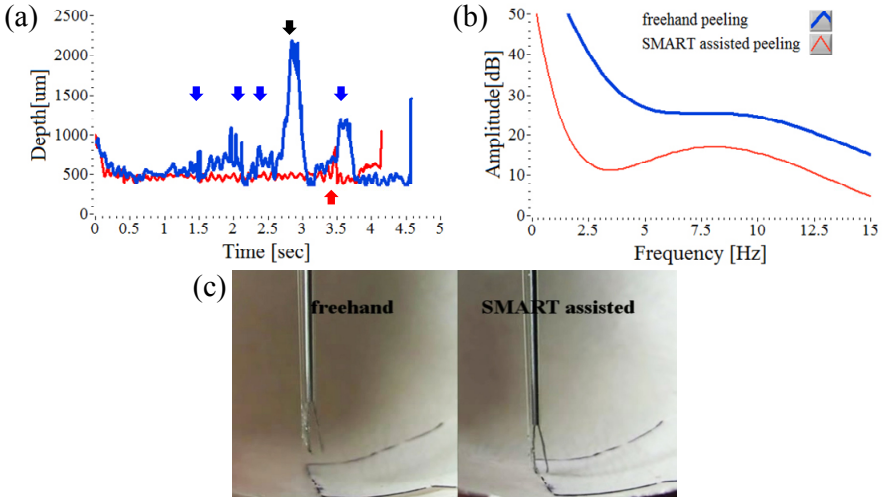

Fig. 5. Comparison of freehand peeling (blue line) and SMART assisted peeling (red line) on the egg shell. (a) Continuous attempts to peel the membrane at a defined offset height of 500 µm. Each arrow indicates the moment of a grasp and the black arrow indicates a next attempt. (b) The Fourier analysis of two height signals, (a). (c) Real-time video image (Media 2) shows a comparison between freehand and SMART assisted peeling of a thin egg membrane.

5. Conclusion

The present proof-of-concept study examines the potential to incorporate active tremor compensation into an active tool tip, in this case a micro-forceps. The SMART micro-forceps utilizes CP-OCT signals as a high-speed, high-precision distance and motion sensor that is connected via feedback control to a piezoelectric motor. The resulting compensatory axial movements of the tool shaft, stabilize the tool tip position relative to the target position for micro-forceps. This provides active tremor compensation during grasping and peeling functions. The prototype successfully suppresses the hand tremor and stabilizes the tool tip in response to surgeon tremor, device drift, and surgeon initiated tool action. Strategic incorporation of SMART functions into active tool tips such as the micro-forceps can enhance surgical capabilities, safety, and efficiency during microsurgery.

Acknowledgments

The authors would like to thank Prof. Russell H. Taylor at Johns Hopkins University for fruitful discussion. The research reported in this paper was supported by the U.S. National Institutes of Health and the National Eye Institute (NIH/NEI) Grant R01EY021540-01A1, Research to Prevent Blindness (RPB), and by the National Research Foundation of Korea (NRF) grant funded by the Korea government (MSIP) (No. 2011-0030075).